

Applicability of Video Gauge for the Assessment of Track Displacement

M.Gallou¹, M Frost¹, A.El-Hamalawi¹, B.Temple², C.Hardwick²

¹Loughborough University, UK

²LB Foster Rail Technologies UK

Numerous techniques have been used for the measurement of the track displacements and consequently the assessment of track stiffness. Some of the most commonly employed are linear variable displacement transducers (LVDTs), geophones and older video monitoring techniques based on Particle Image Velocimetry (PIV). In this paper, the application of the Video Gauge, a relatively new technique, is investigated. This technique can be seen as a quick and reliable way to capture data of high quality and resolution, which can be directly employed for the evaluation of track displacement and hence stiffness. The Video Gauge is used at three different track sites measuring different ballasted track components under various train speeds and types.

1 INTRODUCTION

Understanding track stiffness is vital property for the design and maintenance of railway track structures. Its evaluation is important to assess track quality, component performance, localised track faults and to optimise maintenance periods and activities. In addition its evaluation can help in the investigation of the performance of novel trackforms, as well as the validation of numerical models. Track stiffness may be affected by many factors including track component; condition, ballast condition, by unsupported sleepers, discontinuities of rail bending stiffness (i.e. rail joints), transition zones from a ballasted track to slab systems (bridges and tunnels), as well as condition of the substructure layers. These factors can induce variations in the wheel-rail contact forces and affect the deterioration rate of track geometry and components (1).

Track system stiffness can be estimated by measuring track system displacement and calculating the stiffness from the applied load (a direct approach) or by measuring deflection (via velocity) of a sleeper using a falling weight deflectometer (FWD), and evaluating trackbed stiffness per sleeper end (an indirect approach). Direct displacement methods employ techniques, such as linear variable displacement transducers (LVDTs) (2), laser deflectometers (2, 3) and remote video monitoring using PIV (4,5) and Digital Image Correlation (DIC) (6, 7). Alternatively displacement can be measured indirectly. Geophones (3-5) have been employed for measuring velocity time histories, which can be transformed to displacements through integration. Similarly accelerometers can be used by integrating the signal twice. The accuracy of all measuring techniques where load is not directly measured but vehicle weight is used depends on the train speed, on the instrument sampling frequency and the amount of the displacement measured.

This paper focuses on the use of Video Gauge (VG) technique (see also section 2) for the measurement of track vertical displacements and the procedure needed for the estimation of track stiffness. The benchmarking of the Video Gauge as a useful system to assess various parameters of the railway system such as dynamic deflection under high speed or in tracks with high train-induced movement, 3d deflection for calculation of lateral effects, strains and forces was previously shown (8). Relevant work conducted with the VG included track behaviour investigation at switches and crossings (9). The current work describes complementary technical results of the VG with an improved methodology (large quantity of data with a larger field of view from shorter distance). The developed strategy of the VG has been deployed on ballasted track components under different train speeds and field conditions.

The Video Gauge was also used to measure the displacement of a rail joint. The rail joint can be considered as a weak point in the railway system, which has been experimentally assessed in the past (10, 11), however for the measurement of rail joint deflections, there is a lack of literature work related to video techniques.

2 METHODOLOGY

The Video Gauge technology is based on digital image correlation (DIC). This compares digital images from frames at different time intervals, by tracking the behaviour of pixel (target) groups between frames. Under external excitation (i.e. dynamic loading), DIC allows the calculation of the displacement of a target with respect to time. Measurements were taken using up to two high speed cameras mounted on surveyor's tripods, in the track cess, at a distance of 2-5.5 m from the measured line. The sampling frequency (frames per second) used during recording were up to 200 Hz with a resolution of under 10 microns. Appropriate lenses were used to provide a field of view up to 6.3m. A typical video image with a target array (fixed or painted) is illustrated in Figure 1. Measurements were performed for several train passages in each location assessed.

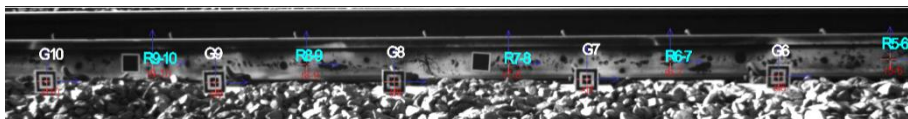


Figure 1 - Typical video image from Site C showing target array on rail web and sleeper edges

Three sites were assessed. The deflection of the rails, sleeper and where possible rail joint were measured. Details are given below:

- (A) A main line with a speed of 40 mph. Here, rail and sleeper displacements were measured simultaneously. The measurements were taken at a sampling frequency of 124 Hz.
- (B) A fast line with a speed of 125 mph. In this case, rail joints displacements were measured and compared with those of adjacent plain rail under the same train passage. The measurements were taken at a sampling frequency of 75 Hz.
- (C) A fast line on a transition zone (approach to a railway bridge) with a speed of 125 mph. Here, rail and sleeper displacements were measured under high speed train passages. A total track length of 6.3 m was measured in this case. The measurements were taken at a sampling frequency of 175 Hz.

While there is some inconsistency in the nature of the sites and trains used, this was down to the availability of sites and safety considerations.

The accuracy of Video Gauge technique depends on the train speed, sampling frequency and the amount of the displacement measured. In particular, the higher the train speed, the higher the displacement frequency for each vehicle. In other words, the possibility to capture the maximum displacements imposed by the wheel passage (load) between two supports depends on the camera's capture rate capability. More information with respect to the train type, speed and wheel loads considered are provided in Table 1.

Table 1– Characteristics of trains monitored

Site	Train type	Speed(mph)	Wheel load (F) (kN)
A	Class 170	40	60
	Pendolino Class 390	125	75
B	Desiro Class 350	72-101	55
	Intercity 225	125	100
C	Intercity 125	125	100

3 THEORETICAL BACKGROUND

The main aim of the paper is to approximate the track stiffness employing the Video Gauge technique. The vertical track stiffness (S_{system}) can be defined as the point load (F) required to produce a unit displacement (δ_{rail}) of the rail measured in kN/mm . This can be considered as the global or composite track stiffness depending on rail flexural rigidity (EI) and on effective support stiffness.

$$S_{system} = \frac{F}{\delta_{rail}} \quad (Eq. 1)$$

The term modulus (k) is used to describe the line load required to cause a unit deflection and it is defined as load per unit length (MN/m) per unit displacement (δ). The track support system modulus (k_{system}) is related to both the railpad ($k_{railpad}$) and trackbed modulus ($k_{trackbed}$) (Eq.2 (12)). It should be noted that in Eq.2, the rigid sleeper stiffness is omitted as the inertia effects and the ground acceleration have not been considered (a quasi-static analysis) (12). "A quasi-static analysis does not automatically calculate loads that may arise from dynamic effects and assumes that the accelerations of the track structure and the ground are negligible" (12). Dynamic effects due to high P2 forces may have influence the magnitude of the displacements in Site B. P2 forces comprise inertia forces associated with the dynamic response of the unsprung masses to variation of the vertical alignment of the rail.

$$\frac{1}{k_{system}} = \frac{1}{k_{railpad}} + \frac{1}{k_{trackbed}} \quad (Eq. 2)$$

According to Beam on Elastic Foundation theory (12) the rail displacement $w(x)$ can be linked with the track support system modulus (k_{system}) (Eq.3) where L (Eq.4) is the characteristic length from the point load along the rail that the displacement bowl extends (12) this, depends on the rail flexural rigidity (EI), while x describes the longitudinal distance along the track:

$$w(x) = \frac{F}{2k_{system}L} e^{-\frac{x}{L}} \left(\cos\left(\frac{x}{L}\right) + \sin\left(\frac{x}{L}\right) \right) \quad (Eq. 3)$$

$$L = \sqrt[4]{\frac{4EI}{k_{system}}} \quad (Eq. 4)$$

For $x=0$, Eq.3 provides the rail displacement ($w(0)$) for the position where the load is applied, leading to simplification of Eq.1 (Eq.6):

$$w(0) = \delta_{rail} = \frac{F}{2k_{system}L} \quad (Eq. 5)$$

$$S_{system} = 2k_{system}L \quad (Eq. 6)$$

Finally, the spring stiffness of the railpad ($s_{railpad}$) correlates with the railpad modulus through the formula $k_{railpad}=s_{railpad}/\text{sleeper spacing}$ (12). The effect of the railpad is more severe for high trackbed modulus ($k_{trackbed}$) and the overall system modulus (S_{system}) cannot exceed that of the softest component of the trackform.

4 RESULTS AND DISCUSSION

In this section, the results of the measurements conducted in the three track sites (A, B and C), in UK, are presented and discussed. From the measurements, the track stiffness was approximated using the equations described in section 3.

4.1 Site A

The vertical displacements of both the rail and sleeper of a conventional ballasted track were measured. In this site one camera was used. This captured detailed rail and sleeper displacements, over a distance of 1.4 m of track length during the passage of two passenger trains (Class 170). A typical time-displacement plot is illustrated in Figure 2. From this plot, the maximum displacement (average of peaks which show the passage of each individual wheel) was obtained correspondingly for the rail and sleeper position. This was used for the estimation of track stiffness (see Eq.1, section 3). In particular, the maximum rail displacement obtained was $\delta_{railmax}=3.02 \text{ mm}$, while the corresponding track stiffness (S_{system}) was 19.9 kN/mm .

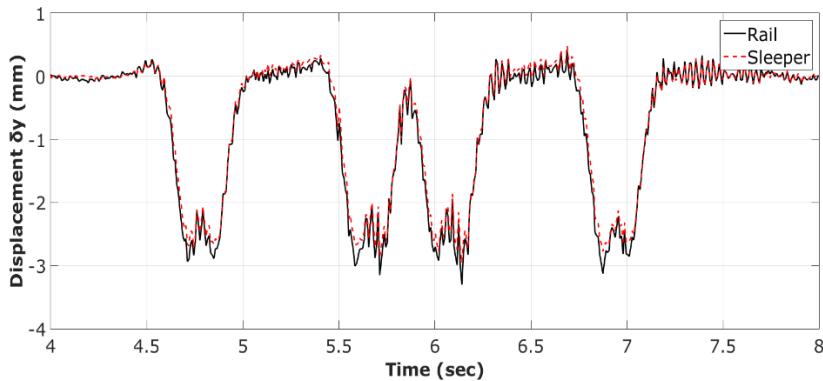


Figure 2 - Vertical displacement time history during the passage of a passenger Cross Country Class 170 train (40 mph)

As mentioned in section 3, the track stiffness depends on the railpad and the trackbed stiffness. Therefore, to estimate the railpad stiffness, the relative displacement between the rail and sleeper ($\delta_{relative}=\delta_{rail}-\delta_{sleeper}$) was calculated (0.34 mm). Then the railpad stiffness ($S_{railpad}$) can be estimated (94.7 kN/mm). This value can be assumed to be realistic, even if it is higher than typical values (60 kN/mm (12)). In addition, the trackbed stiffness was estimated (5.8 kN/mm), which can be assumed to correspond to soft support conditions, as it is lower than the stiffness of a renewed or well-maintained ballasted track (50 kN/mm , (12)).

4.2 Site B

In site B the displacement of a rail joint was measured by the Video Gauge in comparison to the displacement of adjacent plain rail under the passage of five high speed passenger trains (three Pendolino Class 390 and two Desiro Class 350). In this site two cameras were used measuring a distance of $2m$ track length. A typical time-displacement plot for the rail joint and the adjacent plain rail is depicted in Figure 3.

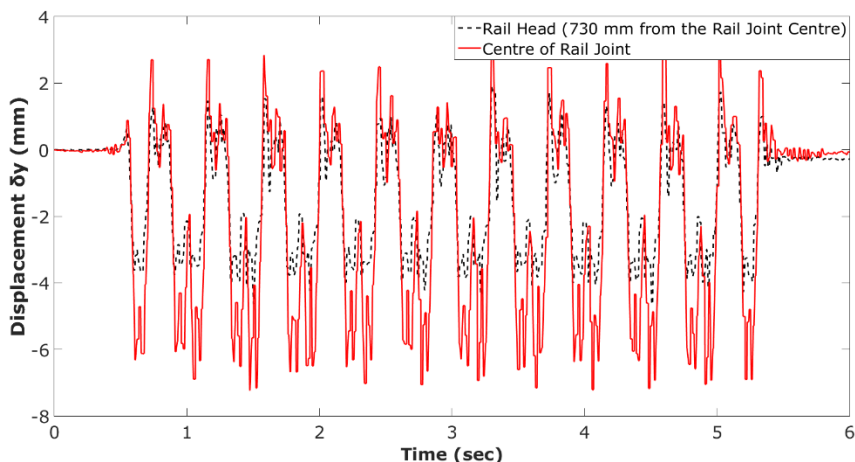


Figure 3– Displacement –time history for rail joint and plain rail during the passage of a Pendolino Class 390 train (125 mph)

Studying the above plot, it can be observed that the rail joint deflects more than the adjacent plain rail (730 mm from the centre of the rail joint). This can be explained by the structural discontinuity, due to the lower section modulus of the joint fishplate, interacting with the wheel impact load. The displacement increment that occurs in the rail joint causes amplification of the dynamic forces induced, which can lead to rail joint and track degradation. Additionally, the positive displacements seen on the plot are assumed to correspond to uplift of the rail ahead of, or behind the wheels. Some differences in amplitude of peak values (that correspond to the passage of each wheel) can be observed. Some of the possible reasons can be variation of vehicle weight (i.e. number of passengers), potential wheel flats (affecting the dynamic forces P_2 induced in the rail) and others. In order to derive the effect of the train speed and axle load on the plain rail and rail joint displacement, the average of all peak values, for each case, was used. This can be seen in Figure 4.

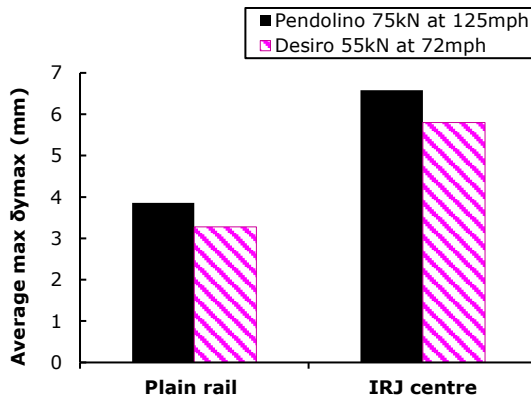


Figure 4- Comparison of average maximum displacements for varying train speed and axle load.

The track stiffness of site B is estimated between $16.8-19.4 \text{ kN/mm}$ according to the maximum rail displacements found for the two train types, that is close to that estimated for site A. The stiffness at the rail joint is estimated around 10.5 kN/mm . Peak displacements could be being amplified due to increased P2 at the joint. Additionally, ineffective discrete support conditions, such as voided sleepers underneath the joint could also increase the joint displacement.

4.3 Site C

At Site C, rail and sleeper displacements were measured in a transition zone from an embankment towards a bridge. Here two cameras were used measuring a distance of 6.3 m of track length under various train passages up to 125 mph . In this case the impact of ineffective sleepers was investigated. In particular, Figure 5 illustrates a typical time-displacement history of two sleepers (G1, G6). From this the increased displacement of the first sleeper against the sixth sleeper is shown. Furthermore, Figure 6 shows the transition zone and the sleeper displacements (based on maximum of each train passage).

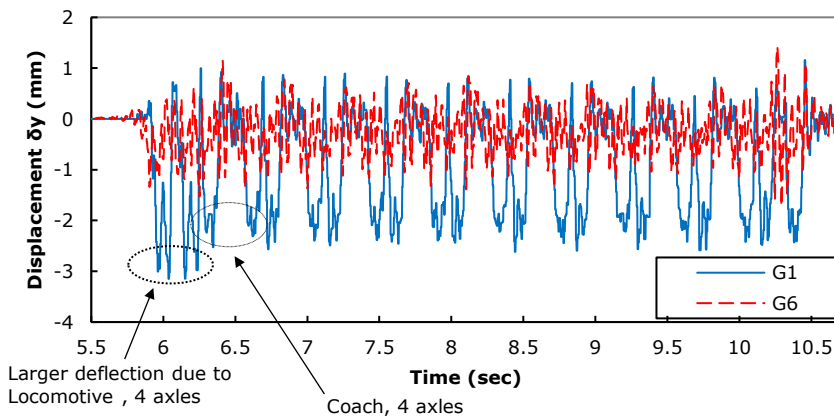


Figure 5- Time-displacement history for the first (G1) and sixth (G6) sleeper in advance of the bridge during Intercity train passage at 125 mph

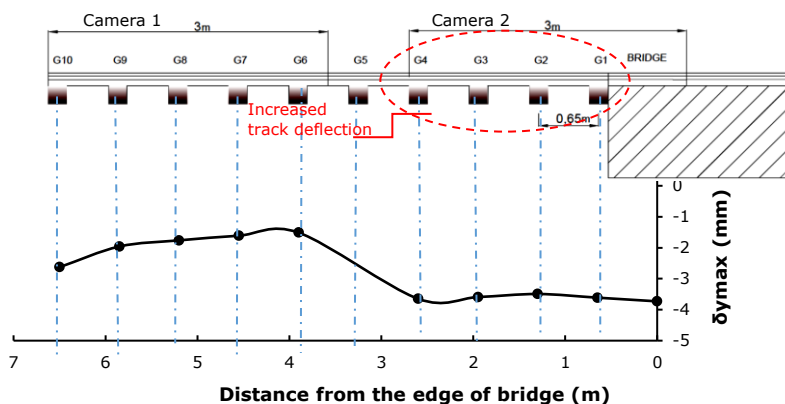


Figure 6 – Transition zone general layout and maximum sleeper dynamic displacements at the approach of an overbridge

Increased deflections were observed on the approach of the bridge. This might have occurred due to track degradation caused by unsupported sleepers with gaps in the sleeper-ballast interface. It should be noted that maintenance work (re-packing of ballast) conducted before the measurements might have influenced the results. At this transition zone (site C) stiffness variation can be associated with drainage problems detected in the embankment, which caused wet beds and sleeper voids. Finally, the stiffness per sleeper end was estimated varying from 27.6 to 61.4 kN/mm which agrees with typical values of trackbeds (12).

5 CONCLUSIONS

In this paper, the Video Gauge, a high definition optical technique for measuring real-time operational dynamic rail-track displacements has been described. A number of field measurements were conducted in the attempt to verify the applicability and reliability of the Video Gauge. In particular, the dynamic displacement histories of different track components were measured, subjected to various train speeds (40-125 mph) and sampling frequencies varying from 75 to 200 Hz (capture rate in frames per second). From the aforementioned investigation it can be concluded that the Video Gauge helped to:

- Acquire displacement data of rail and sleepers for the conventional ballasted track examined.
- Evaluation of track stiffness based on rail and sleeper displacements.
- Acquire displacement data of rail joints and estimation of track stiffness at rail joints
- Investigation of the degradation rate of transition zones through the measurements of rail and sleeper displacements as well as an estimation of track stiffness on transition zones.

These show that the Video Gauge can serve as a valuable tool for the assessment of track displacements and provide information about potential deterioration rate of track irregularities and transition zones. Investigation of the impact of the ratio of the noise after the wheel passage to the signal amplitude on measurement accuracy is recommended for future studies. Further testing of various innovative trackforms is planned in order to be used for life prediction and behaviour assessment.

Acknowledgements

The authors wish to thank the EPSRC for providing funding through the Centre for Innovative Construction Engineering (CICE) at Loughborough University and LB Foster Rail Technologies (UK) Limited for funding and supporting this research project. The authors are grateful to Network Rail (Peter Musgrave) for supporting part of the onsite measurements.

REFERENCE LIST

1. Dahlberg T. Railway Track Stiffness Variations – Consequences and Countermeasures. *Int J Civ Eng*. 2010;8(1):1–12.
2. Farritor S, Fateh M. Measurement of Vertical Track Deflection from a Moving Rail Car. TRID. Report, University of Nebraska, USA, 2013.
3. Innotrack. Methods of track stiffness measurements. Report, Deliverable D2.1.11 for Innotrack project, Project no.TIP5-CT-2006-031415; 2006.
4. Burrow M, Priest M, Ghataora G.S, et al. Track subgrade performance and monitoring. In: *Railway Engineering -9th International Conference and Exhibition*. London, UK, 20-21 June 2007.
5. Bowness D, Lock A, Powrie W, et al. Monitoring the dynamic displacements of railway track. *Proc Inst Mech Eng Part F J Rail Rapid Transit*. 2007;221(1):13–22.
6. Murray C. *Dynamic monitoring of rail and bridge displacement using digital image correlation*. Master Thesis, Queen’s University, Canada, 2013.
7. Thompson II H., Sussmann TR Jr, Stark TD, et al. Non-invasive monitoring of track system gaps. *Railway Engineering - 13th International Conference & Exhibition*. Edinburgh, UK, 30 June-1 July 2015.
8. Waterfall P, Temple B, Hardwick C, et al. Video Measurement techniques for understanding wheel- induced lateral forces and track component deflections. In: *The Stephenson Conference-Research for Railways*. London, UK; 21-23 April 2015.
9. Liu, X., Markine, V. L., & Shevtsov, I. Dynamic experimental tools for condition monitoring of railway turnout crossing. In: *The Second International Conference on Railway Technology: Research, Development and Maintenance*. Ajaccio, Corsica, France, 8-11 April 2014.
10. Askarinejad H, Dhanasekar M, Cole C. Assessing the effects of track input on the response of insulated rail joints using field experiments. *Proc Inst Mech Eng Part F J Rail Rapid Transit*. 2012 Sep 13;227(2):176–87.
11. Soylemez E, Ciloglu K. Influence of Track Variables and Product Design on Insulated Rail Joints. *Transp Res Rec J Transp Res Board*. 2016 Jan;2545:1–10. 1.
12. Powrie W, Le Pen L. A Guide to Track Stiffness. Cross Industry Track Stiffness Working Group; UK; August 2016.